European Journal of Pharmacology 908 (2021) 174336

Contents lists available at ScienceDirect

European Journal of Pharmacology

journal homepage: www.elsevier.com/locate/ejphar

Astaxanthin prevents mitochondrial impairment in the dopaminergic SH-SY5Y cell line exposed to glutamate-mediated excitotoxicity: Role for the Nrf2/HO-1/CO-BR axis

Flávia Bittencourt Brasil [a], Fhelipe Jolner Souza de Almeida [b,c], Matheus Dargesso Luckachaki [c], Evandro Luiz Dall'Oglio [c], Marcos Roberto de Oliveira [c,*]

[a] Departamento de Ciências da Natureza, Campus Universitário de Rio das Ostras – Universidade Federal Fluminense (UFF), Rio de Janeiro, Brazil
[b] Programa de Pós-Graduação em Ciências da Saúde (PPGCS), Universidade Federal de Mato Grosso (UFMT), Cuiaba, MT, Brazil
[c] Grupo de Estudos em Neuroquímica e Neurobiologia de Moléculas Bioativas, Departamento de Química, Universidade Federal de Mato Grosso (UFMT), Av. Fernando Corrêa da Costa, 2367, CEP 78060-900, Cuiaba, MT, Brazil

ARTICLE INFO

Keywords:
Astaxanthin
Nrf2
HO-1
Mitochondria
Bioenergetics
Antioxidant

ABSTRACT

Mitochondrial dysfunction has been viewed in several diseases, including neurological disorders. In the glutamate (GLU)-mediated excitotoxicity, it has been described mitochondrial impairment, disrupted redox environment, and increased rates of cell death in the affected brain areas. Astaxanthin (AST) is a potent antioxidant and anti-inflammatory xanthophyll that also promotes beneficial mitochondria-related effects in brain cells. However, it is not completely clear how AST would be able to promote mitochondrial protection in those cell types. Thus, we investigated here how AST would protect mitochondria in the dopaminergic SH-SY5Y cell line exposed to GLU. AST was administrated to the cells at 1–40 μM for 24 h prior to the exposure to GLU at 80 mM for additional 24 h. AST prevented the GLU-induced impairment in the activity of the Complexes I and V, the loss in mitochondrial membrane potential (MMP), and the decline in the synthesis of ATP. AST also induced an antioxidant effect in the membranes of mitochondria obtained from the GLU-treated SH-SY5Y cells. Inhibition of the enzyme heme oxygenase-1 (HO-1) or silencing of the transcription factor nuclear factor erythroid 2-related factor 2 (Nrf2) suppressed the AST-promoted cellular and mitochondrial protection. Either tricarbonyldichlororuthenium(II) dimer (CORM-2, a source of carbon monoxide - CO) or bilirubin (BR), that are products of the HO-1-biliverdin reductase (BVR) axis, blocked some of the effects caused by GLU in the SH-SY5Y cells. Overall, our data demonstrate that AST prevented mitochondrial dysfunction by a mechanism related to the Nrf2/HO-1 axis in GLU-challenged cells.

1. Introduction

Mitochondria are the most important organelles involved in the maintenance of the bioenergetics status in mammalian cells due to the presence of the oxidative phosphorylation (OXPHOS) system (Papa et al., 2012). The OXPHOS system comprises the electron transfer chain (ETC, *i.e.* the Complexes I - IV and the mobile electron transfer components ubiquinone and cytochrome *c*) and the Complex V (ATP synthase/ATPase) (Papa et al., 2012). In that context, mitochondria are the major source of adenosine triphosphate (ATP) in nucleated cells (Bonora et al., 2012). The consumption of oxygen gas (O_2) by the Complex IV is obligatory to the maintenance of the electron flux in the ETC, since this event is necessary to the generation of an electrochemical gradient across the inner mitochondrial membrane (IMM) that is utilized by Complex V to synthetize ATP (Madeira, 2012). Impairment in the flux of electrons in the ETC affects both production of ATP and the generation of reactive oxygen species (ROS) by the mitochondria (Kausar et al., 2018). Actually, the mitochondria are the main source of ROS in mammalian cells (Kausar et al., 2018). The production of the ROS radical anion superoxide ($O_2^{\bullet-}$) and hydrogen peroxide (H_2O_2) is constant in the mitochondria and may be enhanced by different aspects, such as observed in neuropathological conditions, such as excitotoxicity induced by glutamate (GLU) (Rego and Oliveira, 2003). Abnormal GLU-mediated signaling, mainly as consequence of increased levels of

* Corresponding author.
E-mail addresses: mrobioq@gmail.com, mrobioq@yahoo.com.br (M.R. de Oliveira).

https://doi.org/10.1016/j.ejphar.2021.174336
Received 18 May 2021; Received in revised form 22 June 2021; Accepted 11 July 2021
Available online 13 July 2021
0014-2999/© 2021 Elsevier B.V. All rights reserved.

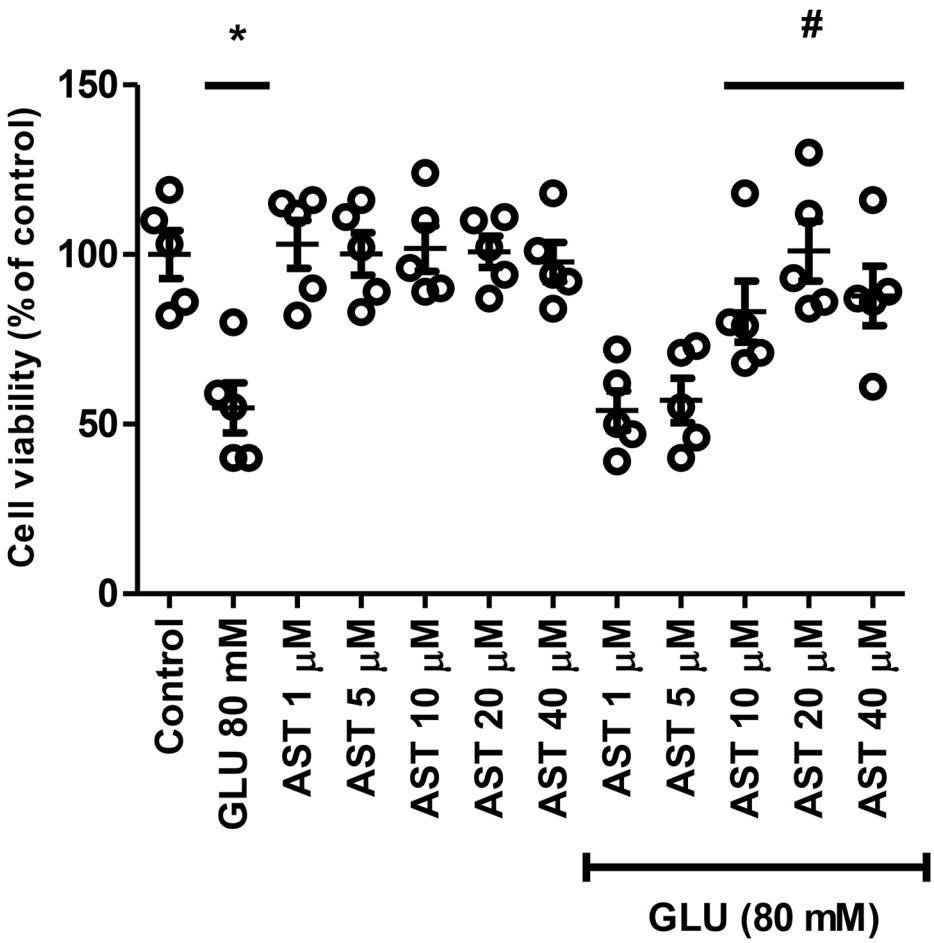

Fig. 1. The effects of astaxanthin (AST) and/or glutamate (GLU) on the viability of the SH-SY5Y cells. AST was administrated to the cells at 20 μM for 24 h before the exposure to GLU at 80 mM for additional 24 h. The data are presented as the mean ± S.E.M. of five independent experiments each done in triplicate. One-way ANOVA followed by the post hoc Tukey's test, *$p < 0.05$ vs control cells, #$p < 0.05$ vs GLU-treated cells.

extracellular GLU, leads to enhanced production of ROS by the mitochondria in calcium ions (Ca^{2+})-associated manner (Duan et al., 2007). Enhanced levels of ROS and of Ca^{2+} ions triggers the intrinsic apoptotic pathway (which is dependent on the mitochondria) in certain cell types, causing increased rates of cell death in the affected brain areas (Duan et al., 2007). The complete mechanism by which GLU-mediated excitotoxicity affects the function of neurons and glia in humans suffering from epilepsy, for example, is not known. Moreover, it has been described that a number of patients (20–30%) may present drug resistance regarding the treatment for epilepsy (Schmidt and Schachter, 2014). Thus, it would be strategic to find new molecules that would be useful in the treatment of epilepsy by modulating mitochondrial physiology, since the complex scenario of events involving these organelles compromises cell survival and affects the life quality of the patients (Baranowski, 2018; Olloquequi et al., 2018).

Astaxanthin (AST; $C_{40}H_{52}O_4$) is xanthophyll found in microalgae and salmon, among other sources, that exhibits potent antioxidant, anti-inflammatory, and anti-atherosclerotic properties in different experimental models (Wang et al., 2010; Wu et al., 2015; Li et al., 2020a, b). AST modulates signaling pathways associated with the control of cell survival, redox biology, and bioenergetics status (Wu et al., 2015). Mohaghegh Shalmani et al. (2020) have shown that AST combined with epidermal neural crest stem cells activated mitochondrial biogenesis in an experimental model of spinal cord injury in rats. García et al. (2020) demonstrated that AST decreased the production of $O_2^{-\bullet}$ by the mitochondria of SH-SY5Y cells exposed to N-methyl-D-aspartate (NMDA), a compound that is utilized to induce excitotoxicity experimentally. Recently, Zhang et al. (2020) reported that AST upregulated the phosphoinositide 3-kinase (PI3K)/Akt/glycogen synthase kinase 3 beta (GSK3β) signaling pathway, leading to the activation of the transcription factor nuclear factor erythroid 2-related factor 2 (Nrf2) in SH-SY5Y cells exposed to oxygen and glucose deprivation. Nrf2 is the master regulator of the redox environment in mammalian cells by controlling the expression of several antioxidant enzymes, such as glutathione peroxidase (GPx), glutathione reductase (GR), γ-glutamate-cysteine ligase (γ-GCL), NAD(P)H dehydrogenase [quinone] 1 (NQO1), and heme oxygenase-1 (HO-1) (Wakabayashi et al., 2010; Ma, 2013). HO-1 has attracted the attention of several research groups due to the potent beneficial effects this enzyme induces in different cell types (de Oliveira et al., 2018; Fürstenau et al., 2019; Gao et al., 2020; Li et al., 2020a, b). HO-1 degrades heme generating iron ions, carbon monoxide (CO), and biliverdin (BV) (Ma, 2013). BV is converted into bilirubin (BR) by the enzyme biliverdin reductase (BVR) (Baranano et al., 2002). The products of the reactions mediated by HO-1 and BVR have been reported to be important cytoprotective agents in cells exposed to a panoply of stressful conditions (Rochette et al., 2018).

In spite of the several efforts to understand how AST affects cellular function and dynamics, the mechanism of action by which AST promoted mitochondria-related cytoprotection in mammalian cells was not sufficiently clarified yet. Thus, we investigated here whether the Nrf2/HO-1 axis would be involved in the mitochondrial protection promoted by AST in an experimental model of GLU-induced excitotoxicity in SH-SY5Y cells.

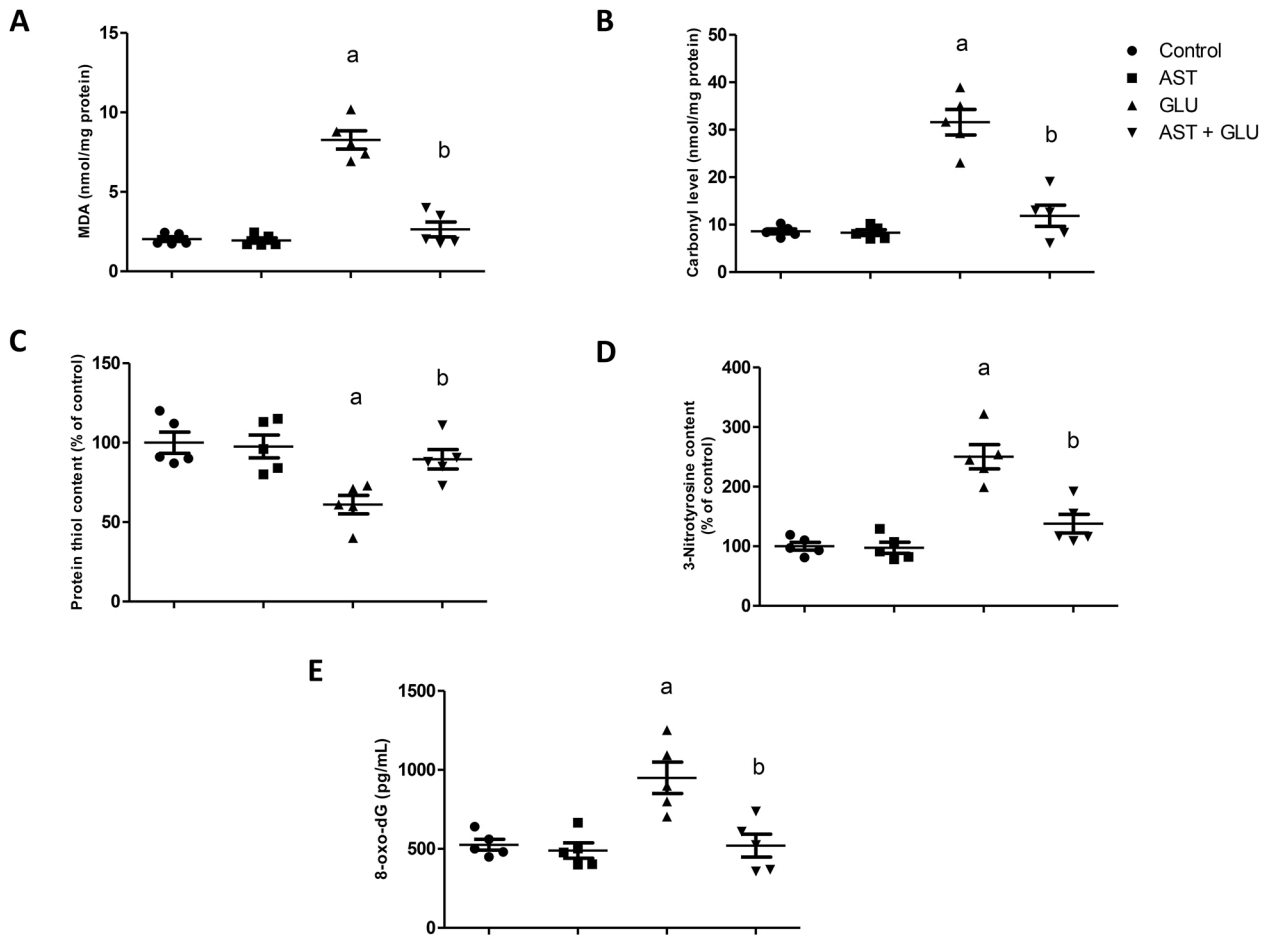

Fig. 2. The effects of astaxanthin (AST) and/or glutamate (GLU) on the levels of malondialdehyde (MDA) (A), protein carbonyl (B), protein thiol (C), 3-nitrotyrosine (D), and 8-hydroxy-2-deoxyguanosine (8-oxodG) (E) in the SH-SY5Y cells. AST was administrated to the cells at 20 μM for 24 h before the exposure to GLU at 80 mM for additional 24 h. The data are presented as the mean ± S.E.M. of five independent experiments each done in triplicate. One-way ANOVA followed by the post hoc Tukey's test, a $p < 0.05$ vs control cells, b $p < 0.05$ vs GLU-treated cells.

2. Material and methods

2.1. Materials

We have acquired AST from Abcam (MA, USA). The analytical grade reagents, Ham's F-12 nutrient mixture, and routine chemicals were obtained from Sigma Chemical Co. (MO, USA). We have purchased plastic materials utilized to maintain cell culture from Corning, Inc. (NY, USA) and Beckton Dickson (NJ, USA). Dulbecco's modified Eagle medium (DMEM) was acquired from Gibco/BRL (Grand Island, USA). The assay kits used here were obtained from Abcam (MA, USA), Cayman Chemical (MI, USA), Roche (Germany), or Promega Corporation (WI, USA), as described below.

2.2. Cell culture

We have purchased the human dopaminergic neuroblastoma SH-SY5Y cells from the American Type Culture Collection (Manassas, VA, USA). The cells were cultured in Dulbecco's modified Eagle's medium (DMEM)/F-12 HAM nutrient medium (1:1 mixture) supplemented with 10% fetal bovine serum (FBS), L-glutamine (2 mM), penicillin (1,000 units/mL), streptomycin (1,000 μg/mL), and amphotericin B (2.5 μg/mL) in a 5% CO_2 humidified incubator (37 °C).

2.3. Treatments

GLU at 80 mM was utilized to induce a 50%-decline in the viability of the SH-SY5Y cells, as previously reported by us (de Oliveira et al., 2019) and by other research groups (Sun et al., 2010; Cunha et al., 2016). Prior to the administration of AST, culture medium was changed to DMEM/F-12 HAM supplemented with 1% FBS overnight. After the exposure to AST for 24 h, the culture medium was replaced and the cells were challenged with GLU. AST was dissolved in DMSO (final concentration < 0.1%) and tested at 1–40 μM for 24 h before the exposure to GLU for further 6 or 24 h, depending on the assay. The specific inhibitor of HO-1, zinc protoporphyrin-IX (ZnPP-IX), was administrated to the cells at 10 μM for 1 h prior to the treatment with AST. Tricarbonyldichlororuthenium(II) dimer (CORM-2) or BR were administrated to the cells at 50 nM for 24 h in the presence or absence of GLU. The transcription factor Nrf2 was silenced by performing cell transfection with Lipofectamine RNAiMAX Reagent (Life Technologies, CA, USA) and small interfering RNA (siRNA) targeting the Nrf2 sequence or with siRNA against non-target mRNA (*i.e.*, the scrambled sequence), based on the protocol provided by the manufacturer (Santa Cruz, CA, USA).

2.4. Cell viability and mitochondria-related apoptotic parameters

Cell viability was assayed by utilizing an assay kit based on the reagent MTT (3-(4,5-dimethylthiazol-2-yl)-2,5-diphenyltetrazolium bromide), based on the protocol provided by the manufacturer (Abcam, MA, USA). The levels of Bax, Bcl-2, and cleaved poly [ADP-ribose] polymerase (PARP) were checked by using a commercial assay kit according to the instructions of the manufacturer (Abcam, MA, USA). The amounts of cytochrome *c* in both cytosolic and mitochondrial fractions

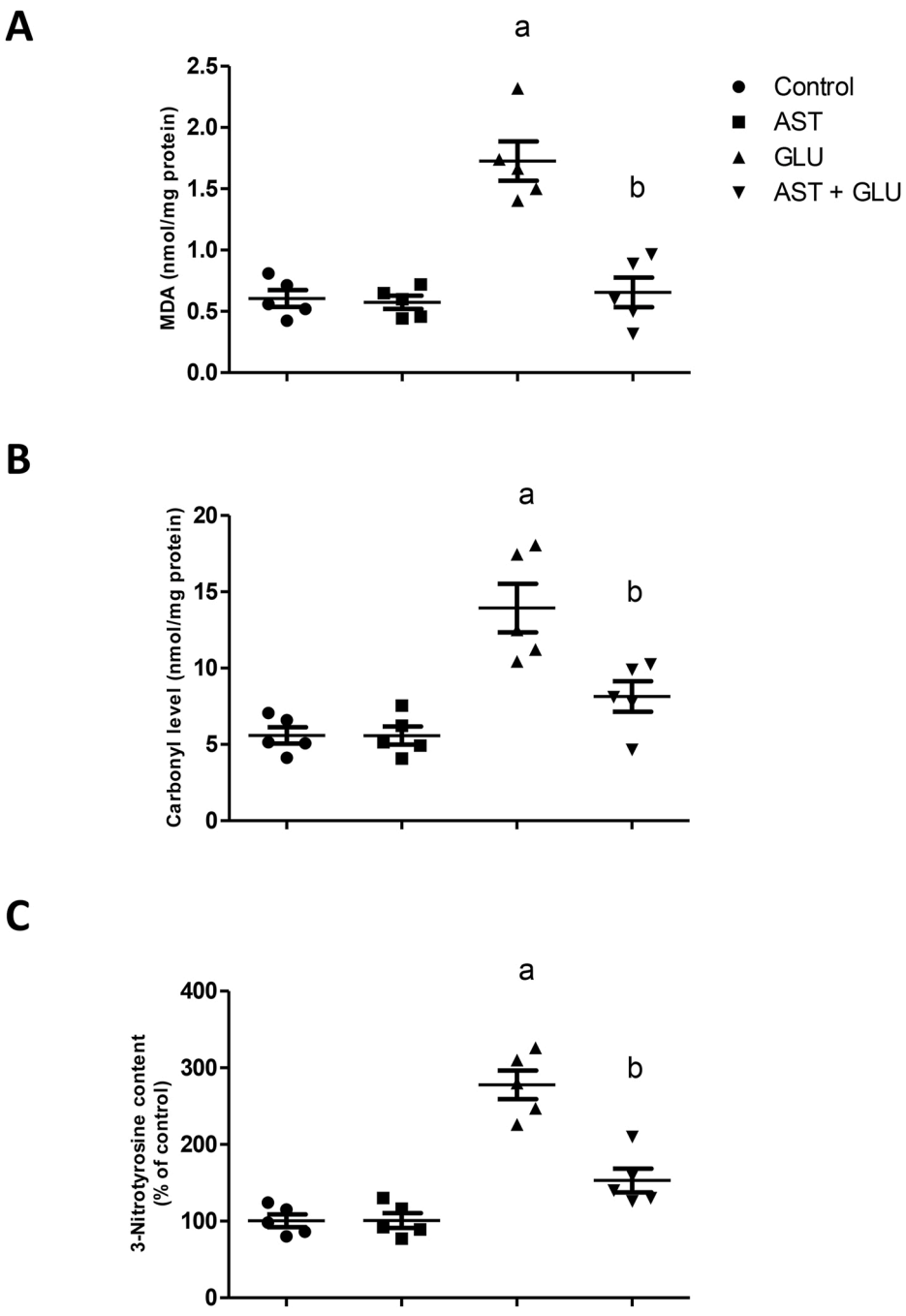

Fig. 3. The effects of astaxanthin (AST) and/or glutamate (GLU) on the levels of malondialdehyde (MDA) (A), protein carbonyl (B), and 3-nitrotyrosine (C) in the membranes of mitochondria isolated from the SH-SY5Y cells. AST was administrated to the cells at 20 μM for 24 h before the exposure to GLU at 80 mM for additional 24 h. The data are presented as the mean ± S.E.M. of five independent experiments each done in triplicate. One-way ANOVA followed by the post hoc Tukey's test, a $p < 0.05$ vs control cells, b $p < 0.05$ vs GLU-treated cells.

were quantified according to the assay described by Borutaite et al. (1999). Briefly, cytochrome *c* levels were measured according to the recording of an ascorbate-reduced-minus-ferricyanide-oxidized absorption difference spectrum (estimation done via the wavelength pairs 550/535 nm, $\varepsilon = 18.5\ mM^{-1}\ cm^{-1}$ for cytochrome *c*, as published by Rieske, 1967). Caspase-9 activity was quantified according to the protocol provided by the manufacturer of an assay kit (Abcam, MA, USA). The cells (1×10^6 cells) were lysed to react with the specific substrate LEDH-AFC (AFC: 7-amino-4-trifluoromethyl coumarin) during 1 h (37 °C). After this step, the signal was recorded at 400 nm (EX) and 505 nm (EM) in a plate fluorometer. Caspase-3 activity was studied in similar conditions. Nonetheless, it was utilized the specific substrate DEVD-AFC. The signal was recorded in a plate fluorometer (EX = 400 nm; EM = 505 nm). It was utilized serial dilutions of the caspases enzymes incubated with their specific substrates to calculate the data, as recommended by the manufacturer. The levels of DNA fragmentation were accessed through the utilization of a commercial assay kit, as described by the manufacturer (Roche, Germany). This assay involves the utilization of 5′-bromo-2′-deoxy-uridine (BrdU), a thymidine analogue. BrdU is incorporated in the genomic DNA and, after fragmentation, the BrdU-labeled DNA fragments are detected in the cytoplasm by using an anti-BrdU antibody. The signal was recorded at 370 nm in a plate spectrophotometer.

2.5. Redox stress markers

We studied the levels of malondialdehyde (MDA) following the protocol provided by the manufacturer of an assay kit (Abcam, MA, USA). After the recommended incubations, the signal was recorded at 695 nm in a plate spectrophotometer. The levels of protein carbonyl

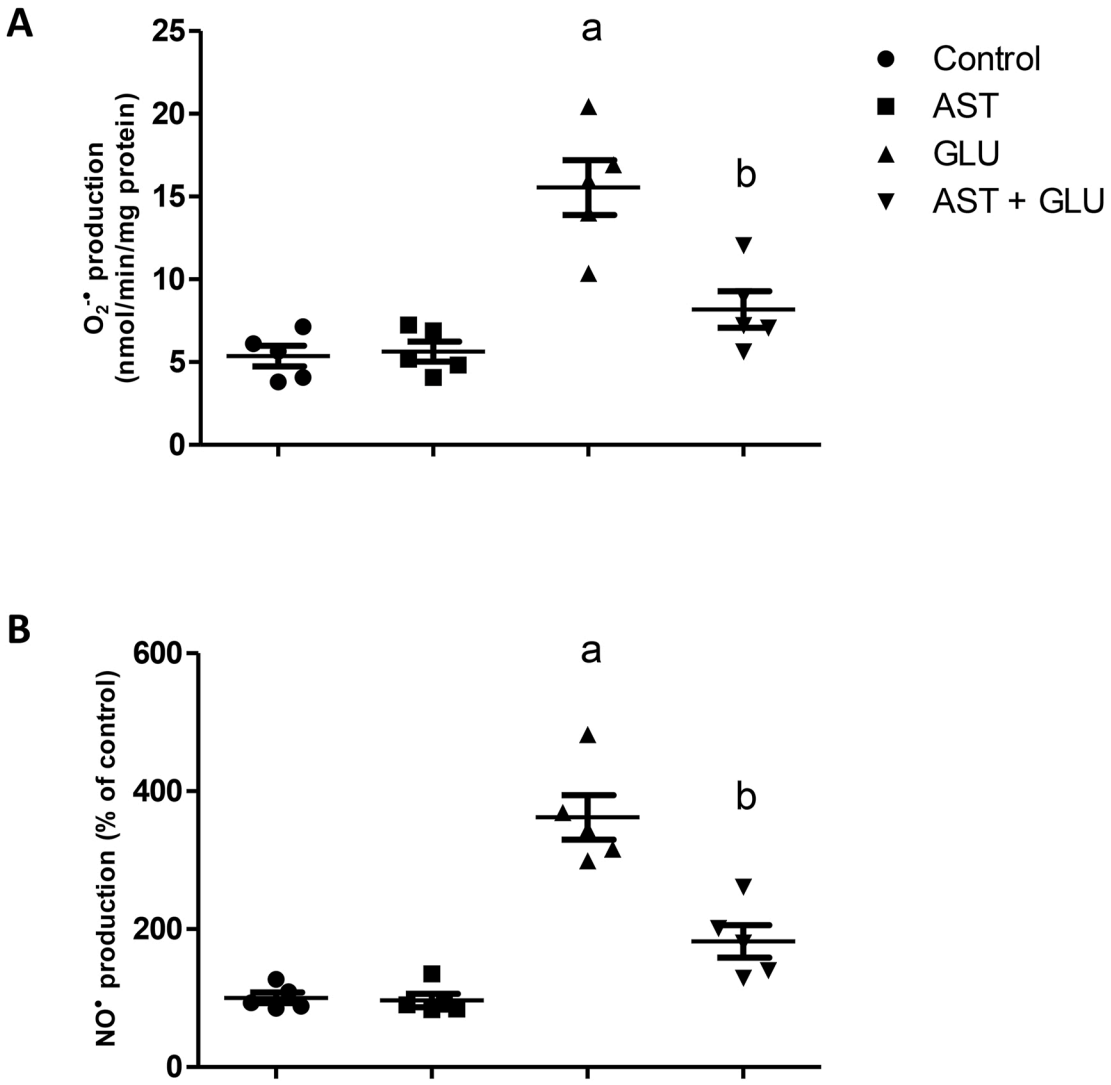

Fig. 4. The effects of astaxanthin (AST) and/or glutamate (GLU) on the production of radical anion superoxide ($O_2^{\bullet-}$) (A) and of nitric oxide ($NO^{\bullet}$) (B) in the SH-SY5Y cells. AST was administrated to the cells at 20 μM for 24 h before the exposure to GLU at 80 mM for additional 6 h. The data are presented as the mean ± S.E.M. of five independent experiments each done in triplicate. One-way ANOVA followed by the post hoc Tukey's test, a $p < 0.05$ vs control cells, b $p < 0.05$ vs GLU-treated cells.

were analyzed after the reaction of the proteins present in the samples with dinitrophenylhydrazine (DNPH). Then, an anti-DNPH antibody was utilized to detect the protein groups in the samples. The signal was recorded at 450 nm in a plate spectrophotometer. The levels of protein thiol groups were checked by using the Thiol Blue reagent, following the protocol provided by the manufacturer (Abcam, MA, USA). The signal was read at 680 nm and 280 nm (the absorbance ratio of 680 nm and 280 nm was utilized to calculate the amount of protein thiol groups). We have utilized an indirect ELISA assay protocol to investigate the levels of 3-nitrotyrosine in the samples (de Oliveira et al., 2015). The amounts of 8-hydroxy-2′-deoxyguanosine (8-OHdG) were quantified by using an assay kit according to the protocol provided by the manufacturer (Abcam, MA, USA). Prior to studying DNA oxidative damage, it was necessary extracting DNA from the cells. Then, we have utilized an assay kit to perform DNA isolation, as recommended by the manufacturer (Promega Corporation, WI, USA).

2.6. Reactive species production

We have studied the production of $O_2^{\bullet-}$ according to the protocol described by Poderoso et al. (1996). The production of $NO^{\bullet}$ was quantified by using a fluorescence probe (2,3-diaminonaphthalene, DAN), according to the protocol provided by the manufacturer of an assay kit (Abcam, MA, USA).

2.7. Mitochondrial isolation

We utilized the protocol published by Wang et al. (2014) to extract mitochondria from the SH-SY5Y cells. We homogenized the cells in a buffer presenting 250 mM sucrose, 10 mM KCl, 1 mM EGTA, 1 mM EDTA, 1 mM $MgCl_2$, 1 mM dithiothreitol, 1 mM phenylmethylsulphonyl floride, 1 mM benzamidine, 1 mM pepstatin A, 10 mg/mL leupeptin, 2 mg/mL aprotonin, and 20 mM HEPES at pH 7.4. After this step, we have centrifuged the samples at 1000×*g* (10 min, 4 °C). The supernantant was centrifuged at 11000×*g* (20 min, 4 °C) and mitochondria were obtained. We have not detected significant activity of the cytosolic enzyme lactate dehydrogenase (LDH) in the mitochondrial and nuclear fractions we have extracted from the SH-SY5Y cells (Figs. S1A and B, respectively). We obtained the submitochondrial particles (SMP; *i.e.*, mitochondrial membranes presenting the OXPHOS system in a functional state) from the SH-SY5Y cells by using the protocol published by Poderoso et al. (1996). SMP may be used to detect the markers of redox impairment in

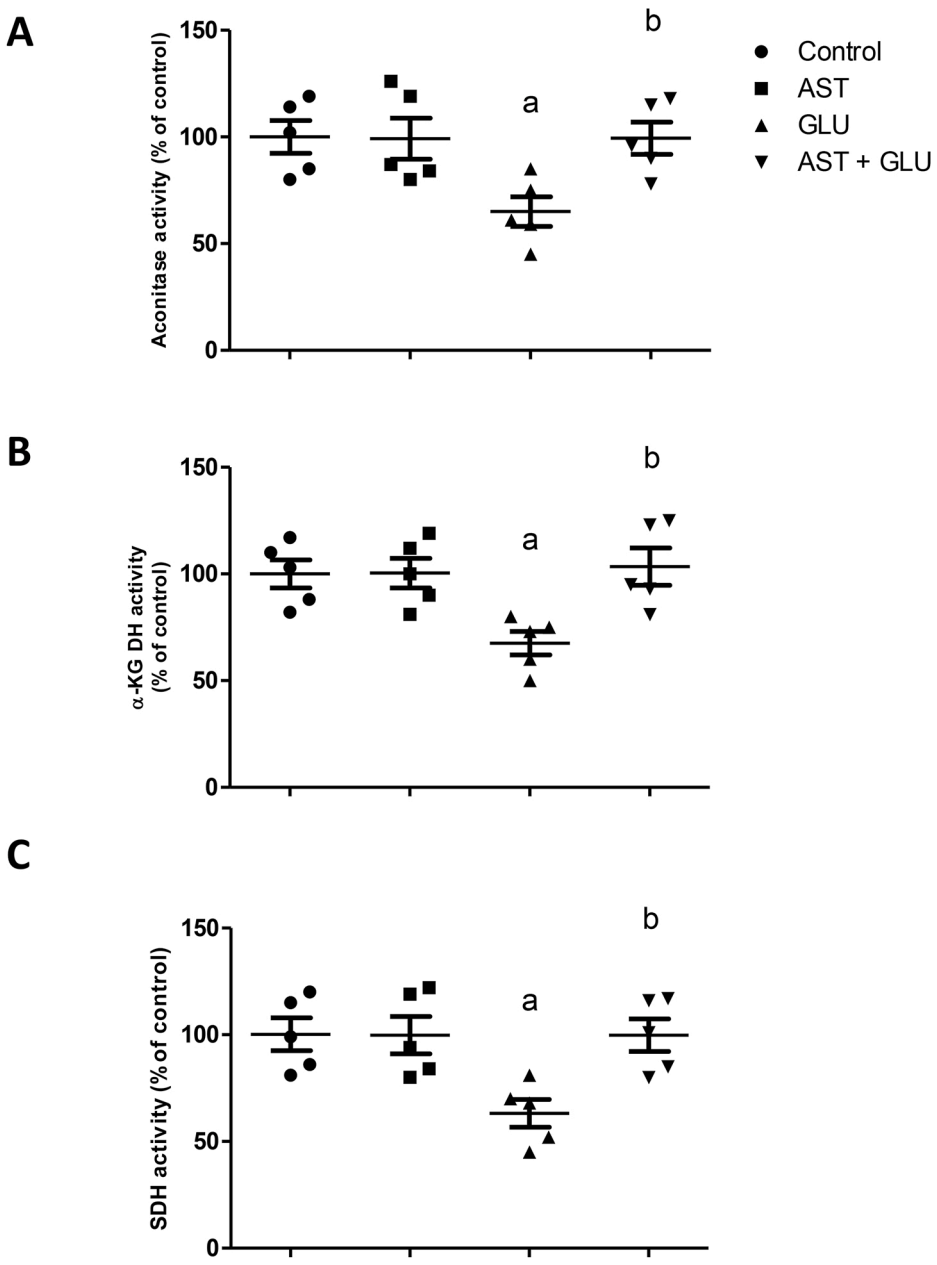

Fig. 5. The effects of astaxanthin (AST) and/or glutamate (GLU) on the activity of the enzymes aconitase (A), α-ketoglutarate dehydrogenase (α-KGDH) (B), and succinate dehydrogenase (SDH) in the SH-SY5Y cells. AST was administrated to the cells at 20 μM for 24 h before the exposure to GLU at 80 mM for additional 24 h. The data are presented as the mean ± S.E.M. of five independent experiments each done in triplicate. One-way ANOVA followed by the post hoc Tukey's test, a $p < 0.05$ vs control cells, b $p < 0.05$ vs GLU-treated cells.

mitochondrial membranes, as well as to quantify the production of $O_2^{-\bullet}$ by the mitochondria, among other experiments focused on the mitochondria.

2.8. Nuclear isolation

After collecting the cells by scraping, the nuclei were isolated following the instructions of the manufacturer of an assay kit (Cayman Chemical, MI, USA). Briefly, 1×10^7 cells were lysed using hypotonic lysis buffer and NP-40 present in the kit. The levels of protein were quantified by the method described by Bradford.

2.9. Mitochondrial function

Aconitase activity was investigated here by utilizing an assay kit based on the recommendations of the manufacturer (Abcam, MA, USA). In this assay, isocitrate is generated from citrate and interacts with a probe whose signal is read at 450 nm in a plate spectrophotometer. The activity of α-ketoglutarate dehydrogenase (α-KGDH) was detected in the samples by using an assay kit based on the recommendations of the manufacturer (Abcam, MA, USA). Briefly, the enzyme converts α-ketoglutarate into an intermediate that interacts with a probe present in the kit, reducing it and generating a colored product whose signal is read at 450 nm in a plate spectrophotometer. A commercial assay kit was also utilized to test the activity of the enzyme succinate dehydrogenase (SDH) following the protocol provided by the manufacturer (Abcam,

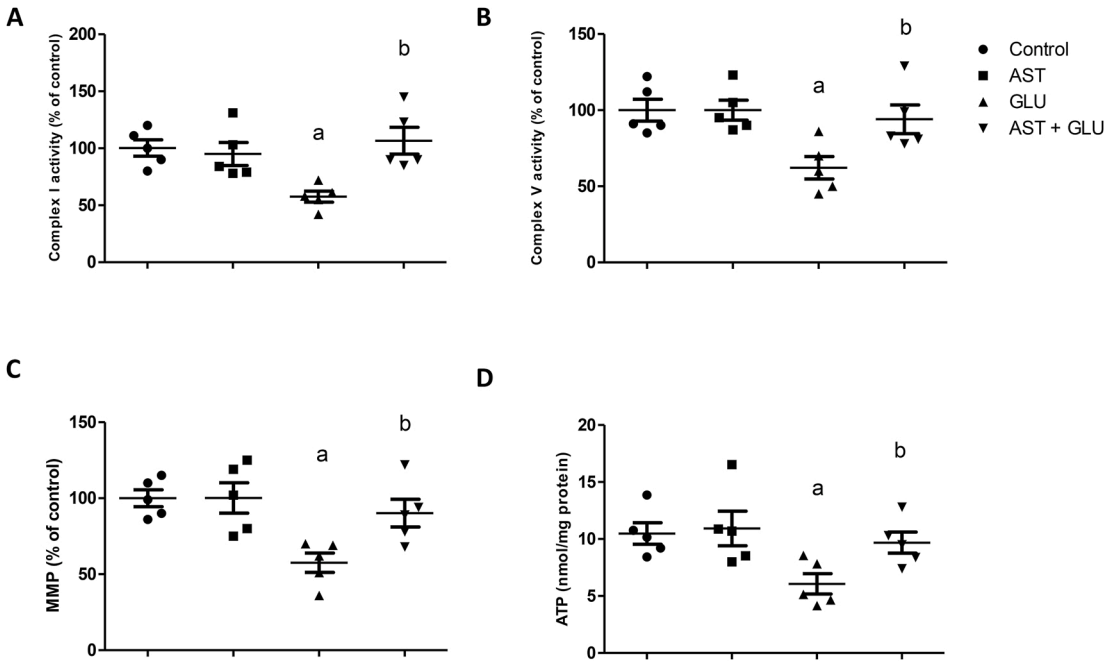

Fig. 6. The effects of astaxanthin (AST) and/or glutamate (GLU) on the activity of the Complexes I (A) and V (B), and on the levels of mitochondrial membrane potential (MMP) (C) and of adenosine triphosphate (AT) (D). AST was administrated to the cells at 20 μM for 24 h before the exposure to GLU at 80 mM for additional 24 h. The data are presented as the mean ± S.E.M. of five independent experiments each done in triplicate. One-way ANOVA followed by the post hoc Tukey's test, a $p < 0.05$ vs control cells, b $p < 0.05$ vs GLU-treated cells.

MA, USA). In brief, SDH generates fumarate from succinate, reducing a probe whose signal was recorded at 600 nm in a plate spectrophotometer. The activity of Complex I was quantified by using a commercially available assay kit according to the protocol provided by the manufacturer (Abcam, MA, USA). This assay kit uses capture antibodies for Complex I pre-coated in the microplate wells. The oxidation of NADH to NAD^+ causes the reduction of a probe and the signal is read at 450 nm in a plate spectrophotometer. The activity of Complex V was also studied by using an assay kit based on the recommendations of the manufacturer (Abcam, MA, USA). Briefly, the ADP generated from ATP by the Complex V-mediated reaction is used by pyruvate kinase to convert phosphoenolpyruvate into pyruvate, generating ATP. In the presence of NADH and lactate dehydrogenase, pyruvate generates lactate and NAD^+. The oxidation of NADH is monitored at 340 nm in a plate spectrophotometer. In order to evaluate the values of mitochondrial membrane potential (MMP), we have utilized the assay kit that contains the dye tetraethylbenzimidazolylcarbocyanine iodide (JC-1), following the instructions of the manufacturer (Abcam, MA, USA). The amounts of ATP were quantified according toh the protocol provided by the manufacturer of an assay kit (Abcam, MA, USA). The phosphorylation of glycerol generates a product whose signal was read at 570 nm in a plate spectrophotometer.

2.10. HO-1 enzyme activity

We have followed the protocol published by Hwang et al. (2008) to evaluate the activity of HO-1 in the SH-SY5Y cells. Briefly, we extracted the microsomal fraction incubated it with 0.2 mM hemin, 0.2 mM $MgCl_2$, purified biliverdin reductase (whose activity was correspondent to 1–1.5 nmol of bilirubin/min/mg protein, as described by Maines, 1990), 2 mM glucose-6-phosphate, 1 U/mL glucose-6-phosphate dehydrogenase, 1 mM NADPH, and 50 mM PBS (pH 7.4) for 2 h (37 °C). Then, chloroform was administrated to the system aiming to stop the reaction. The signal was recorded at 464 nm and 530 nm. The amounts of bilirubin were calculated after obtaining the difference between the values recorded in the two wavelengths.

2.11. Nrf2 activity

We have utilized an assay kit to evaluate the activity of the transcription factor Nrf2 in this experimental model, based on the protocol provided by the manufacturer (Abcam, MA, USA). The nuclei were isolated and the samples were added to the wells of a plate presenting the specific double stranded DNA sequence with the Nrf2 consensus binding site (5′-GTCACAGTGACTCAGCAGAATCTG-3′).

2.12. Statistical analyses

The data were statistically analyzed by using the GraphPad 5.0 software. Data presented here are demonstrated as the mean ± standard error of the mean (S.E.M.) of five independent experiments (performed in triplicate). Values of *p* were considered significant when $p < 0.05$. Data were subjected to statistical analysis by performing the one-way ANOVA analysis followed by the post hoc Tukey's test.

3. Results

3.1. AST prevented the loss of cell viability and the mitochondria-related triggering of cell death induced by GLU

As may be observed in Fig. 1, GLU at 80 mM induced a significant decline in the viability of the SH-SY5Y cells ($p < 0.05$). AST alone did not affect cell viability in this experimental model. AST at 10–40 μM prevented the loss of cell viability induced by GLU on the SH-SY5Y cells (p

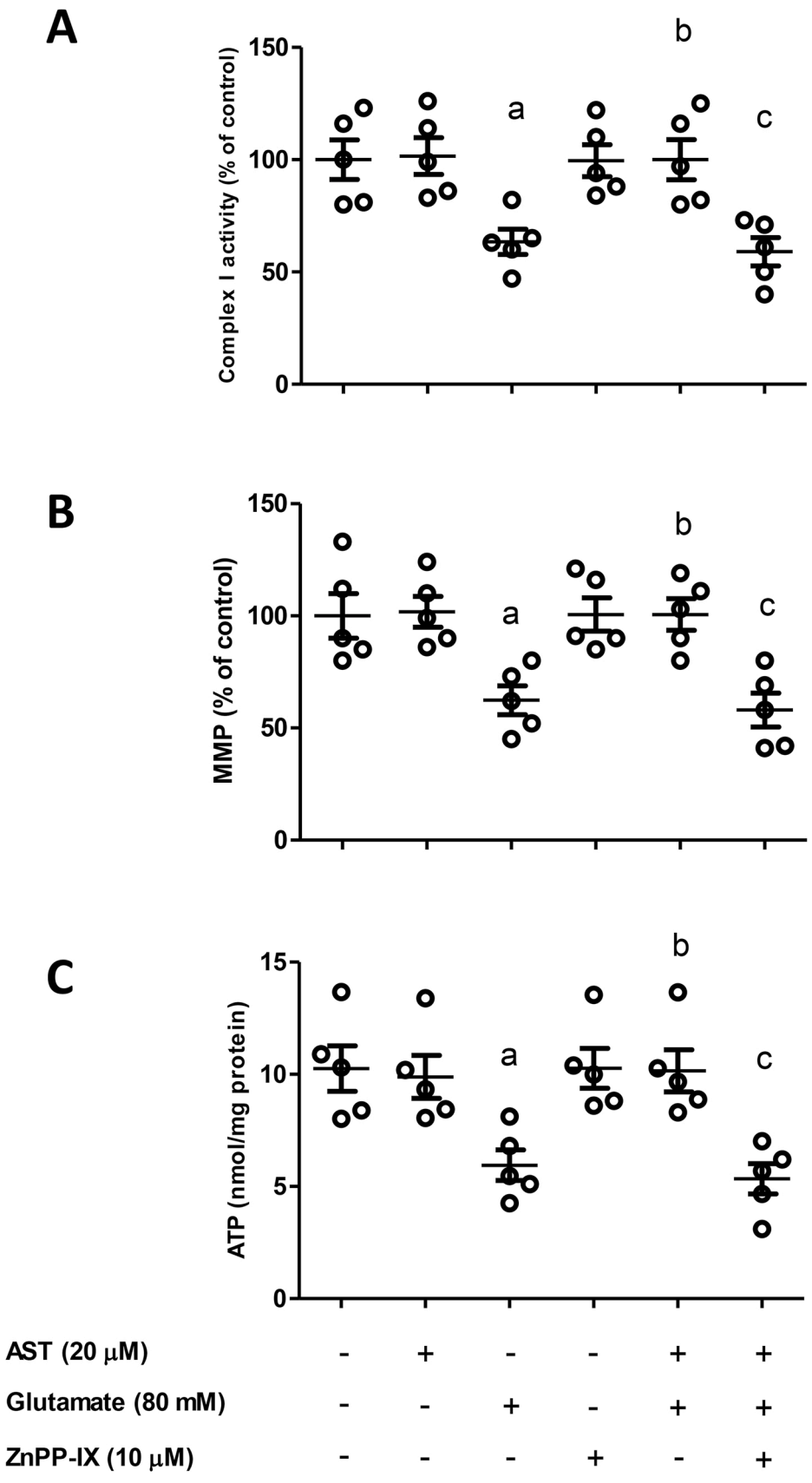

Fig. 7. The effects of zinc protoporphyrin-IX (ZnPP-IX, a specific inhibitor of the enzyme heme oxygenase-1) on the activity of Complex I (A), and on the levels of mitochondrial membrane potential (MMP) (B) and adenosine triphosphate (ATP) (C) in SH-SY5Y cells treated with astaxanthin (AST) and/or glutamate (GLU). The human neuroblastoma SH-SY5Y cells were treated with ZnPP-IX at 10 μM for 1 h prior to the administration of AST at 20 μM for additional 24 h. Then, the cells were challenged with GLU at 80 mM for 24 h after the treatment with AST. The data are presented as the mean ± S.E.M. of five independent experiments each done in triplicate. One-way ANOVA followed by the post hoc Tukey's test, a $p < 0.05$ vs control cells, b $p < 0.05$ vs GLU-treated cells, c vs AST + GLU-treated cells.

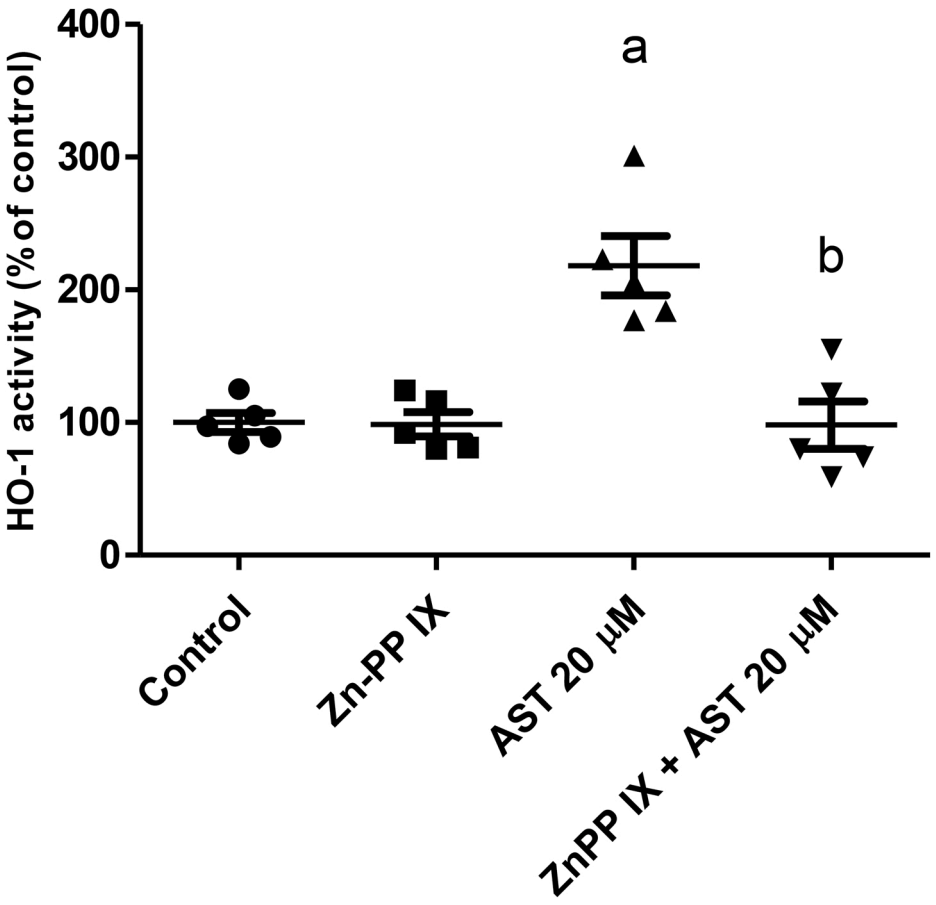

Fig. 8. The effects of astaxanthin (AST) and/or zinc protoporphyrin-IX (ZnPP-IX) on the activity of the enzyme heme oxygenase-1 (HO-1) in the SH-SY5Y cells. The human neuroblastoma SH-SY5Y cells were treated with ZnPP-IX at 10 μM for 1 h prior to the administration of AST at 20 μM for additional 24 h. The data are presented as the mean ± S.E.M. of five independent experiments each done in triplicate. One-way ANOVA followed by the post hoc Tukey's test, a $p < 0.05$ vs control cells, b $p < 0.05$ vs AST-treated cells.

< 0.05). Based on these data and on previously published works (Wang et al., 2010; Zhang et al., 2020), we tested AST at 20 μM in further assays. AST at 20 μM prevented the GLU-induced increase in the levels of the pro-apoptotic protein Bax, as depicted in Fig. S2A ($p < 0.05$). AST pretreatment also blocked the GLU-elicited decrease in the levels of Bcl-2, an anti-apoptotic protein ($p < 0.05$; Fig. S2B). The pretreatment with AST suppressed the effects of GLU on the release of cytochrome *c* from the mitochondria to the cytosol, as may be observed in Figs. S2C and D ($p < 0.05$). Consequently, AST pretreatment blocked the GLU-induced increase in the activity of the pro-apoptotic caspases-9 and -3 in the SH-SY5Y cells ($p < 0.05$; Figs. S2E and F, respectively). AST was also capable to prevent the GLU-induced DNA fragmentation and cleavage of PARP in the SH-SY5Y cells ($p < 0.05$; Figs. S3A and B, respectively).

3.2. AST pretreatment induced an antioxidant effect in the SH-SY5Y cells exposed to GLU

According to Fig. 2A, a pretreatment with AST at 20 μM significantly attenuated the GLU-induced increase in the levels of MDA, which is utilized as an index of lipid peroxidation, in the SH-SY5Y cells ($p < 0.05$). Moreover, the levels of protein carbonylation were also decreased by AST in the GLU-treated cells ($p < 0.05$; Fig. 2B). AST pretreatment also alleviated the GLU-induced decline in the levels of protein thiol in the SH-SY5Y cells, as may be viewed in Fig. 2C ($p < 0.05$). Protein nitration was also prevented by AST in the cells exposed to GLU ($p < 0.05$; Fig. 2D). AST pretreatment significantly reduced the levels of 8-oxo-dG, a marker of DNA oxidation, in the cells challenged with GLU ($p < 0.05$; Fig. 2E). We next examined whether AST would be able to prevent the GLU-induced redox impairment in the membranes of mitochondria obtained from the SH-SY5Y cells. According to Fig. 3A, AST prevented the GLU-induced lipid peroxidation in the membranes of mitochondria isolated from the SH-SY5Y cells ($p < 0.05$). AST was also efficient in attenuating both protein carbonylation and nitration in the membranes of mitochondria extracted from the GLU-treated cells ($p < 0.05$; Fig. 3B and C, respectively). Next, we found that the pretreatment with AST significantly reduced the production of the free radical $O_2^{\bullet}$ by the mitochondria in the cells exposed to GLU ($p < 0.05$; Fig. 4A). Additionally, AST prevented the GLU-promoted increase in the production of $NO^{\bullet}$ in the SH-SY5Y cells ($p < 0.05$; Fig. 4B).

3.3. AST prevented the GLU-induced bioenergetics decline in the SH-SY5Y cells

The pretreatment with AST reduced the impact of GLU on the activity of aconitase, α-KGDH, and SDH, which are enzymes of the tricarboxylic acid cycle ($p < 0.05$; Fig. 5A, B, and C, respectively). AST pretreatment was also capable to decrease the effect of GLU on the activity of the Complexes I and V in this experimental model ($p < 0.05$; Fig. 6A and B, respectively). The pretreatment with AST also suppressed the GLU-induced loss of MMP in the SH-SY5Y cells ($p < 0.05$; Fig. 6C). As demonstrated in Fig. 6D, AST prevented the decline in the levels of ATP in the cells challenged with GLU ($p < 0.05$; Fig. 6D).

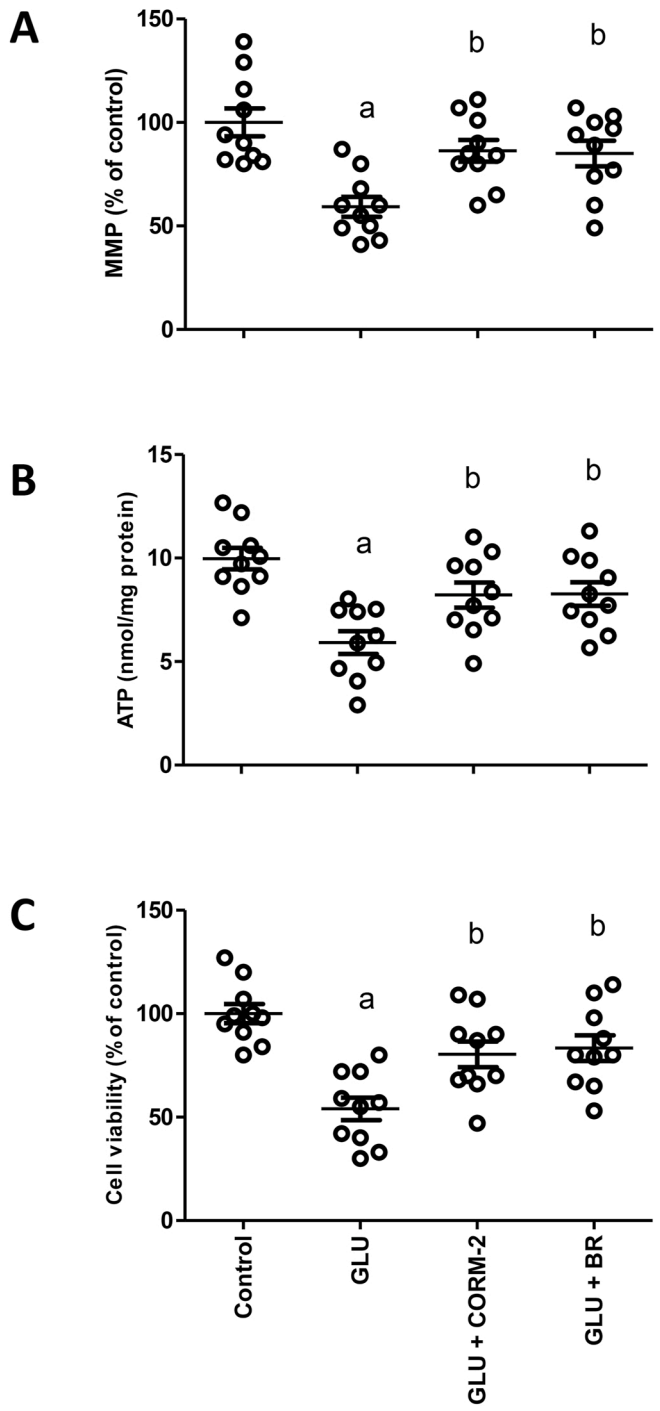

Fig. 9. The effects of glutamate (GLU), tricarbonyldichlororuthenium(II) dimer (CORM-2), and/or bilirubin (BR) on the levels of mitochondrial membrane potential (MMP) (A) and adenosine triphosphate (ATP) and on the viability (C) of the SH-SY5Y cells. Either CORM-2 or BR was administrated to the cells at 50 nM in the presence of GLU at 80 mM for 24 h. The data are presented as the mean ± S.E.M. of ten independent experiments each done in triplicate. One-way ANOVA followed by the post hoc Tukey's test, a $p < 0.05$ vs control cells, b $p < 0.05$ vs GLU-treated cells.

3.4. AST induced cellular and mitochondrial protection by a mechanism dependent on the Nrf2/HO-1 axis in cells exposed to GLU

We next examined the mechanism of action by which AST prevented the GLU-induced cellular and mitochondrial impairments in this experimental model. As may be observed in Fig. 7A, ZnPP-IX, which is a specific inhibitor of the enzyme HO-1, abrogated the effects of AST on the activity of Complex I in the cells exposed to GLU ($p < 0.05$). Similarly, ZnPP-IX suppressed the effect of the pretreatment with AST on the levels of MMP in the cells treated with GLU ($p < 0.05$; Fig. 7B). ZnPP-IX also blocked the effects of AST on the levels of ATP in the cells challenged with GLU ($p < 0.05$; Fig. 7C). As depicted in Fig. S4A, AST failed to prevent the GLU-induced lipid peroxidation in the membranes of mitochondria obtained from the cells that were treated with ZnPP-IX ($p < 0.05$). ZnPP-IX also blocked the effect of the pretreatment with AST on the levels of cytochrome *c* in the mitochondria obtained from the cells exposed to GLU ($p < 0.05$; Fig. S4B). Moreover, inhibition of HO-1 by ZnPP-IX suppressed the effect of AST on the viability of the cells exposed to GLU ($p < 0.05$; Fig. S5). We found that AST at 20 μM significantly upregulated the activity of HO-1 in the SH-SY5Y cells, as demonstrated in Fig. 8 ($p < 0.05$). Administration of ZnPP-IX significantly blocked the effect of AST on the activity of HO-1 in the SH-SY5Y cells, as demonstrated in the same figure ($p < 0.05$). We also checked whether CORM-2 (which generates CO constantly) or BR would be able to prevent some of the impairments caused by GLU in the SH-SY5Y cells. According to Fig. 9, either CORM-2 or BR significantly alleviated the effects of GLU on the levels of MMP and ATP and on the viability of the cells ($p < 0.05$; Fig. 9A, B, and C, respectively). Then, we tested whether the transcription factor Nrf2 would be involved in the modulation of HO-1 in this experimental model. We found that the silencing of Nrf2 by using siRNA against this transcription factor blocked the effect of AST on the activity of HO-1 ($p < 0.05$; Fig. 10A). The activity of Nrf2 was also affected by silencing of this transcription factor in the AST-treated cells, as may be observed in Fig. 10B ($p < 0.05$). Furthermore, silencing of Nrf2 suppressed the effects of AST on the activity of Complex I and on the levels of MMP and ATP in the cells exposed to GLU ($p < 0.05$; Fig. 11A, B, and C, respectively). Nrf2 silencing also blocked the effect of AST on the mitochondrial content of cytochrome *c* in the cells challenged with GLU ($p < 0.05$; Fig. S6). Finally, Nrf2 knockdown suppressed the action of AST on the viability of the SH-SY5Y cells exposed to GLU ($p < 0.05$; Fig. 12).

4. Discussion

In this work, we have found that AST promoted mitochondria-related cytoprotection in SH-SY5Y cells exposed to GLU by a mechanism dependent on the Nrf2/HO-1 axis. The link between the Nrf2/HO-1 signaling pathway and mitochondrial protection was not completely explored before in cells treated with AST. The xanthophyll prevented the redox impairment caused by GLU in both cellular and mitochondrial fractions and preserved the function of the mitochondria. Consequently, AST pretreatment suppressed the bioenergetics failure caused by GLU in the SH-SY5Y cells. Inhibition of the enzyme HO-1 or silencing of the transcription factor Nrf2 abrogated the AST-induced protection. Importantly, either CORM-2 (a source of CO) or BR (the product of the enzyme BVR) counteracted the effects of GLU on certain parameters of mitochondrial function (namely, MMP and ATP levels) and cell viability. CO (a direct product of the reaction mediated by HO-1) and BR (a product generated by the reaction mediated by BVR on BV, a direct product resulting from the reaction mediated by HO-1) exhibit potent antioxidant and anti-inflammatory actions, as assayed in different experimental models (Gozzelino et al., 2010; Rochette et al., 2018). Thus, evidence point to a role for HO-1 in stimulating mitochondrial protection in cells AST-treated cells exposed to GLU. This would be pharmacologically strategic in the case of neurodegenerative diseases, since a vicious cycle involving mitochondrial dysfunction and impaired redox environment (*i.e.* increased production of ROS, enhanced levels of redox stress markers, and altered activity of antioxidant and detoxifying enzymes) is observed in those disorders, leading neurons and glia to undergo cell death (Fricker et al., 2018; Sheeler et al., 2020).

Wang et al. (2010) firstly demonstrated that AST upregulated the enzyme HO-1 in SH-SY5Y cells; however, the link between Nrf2 and

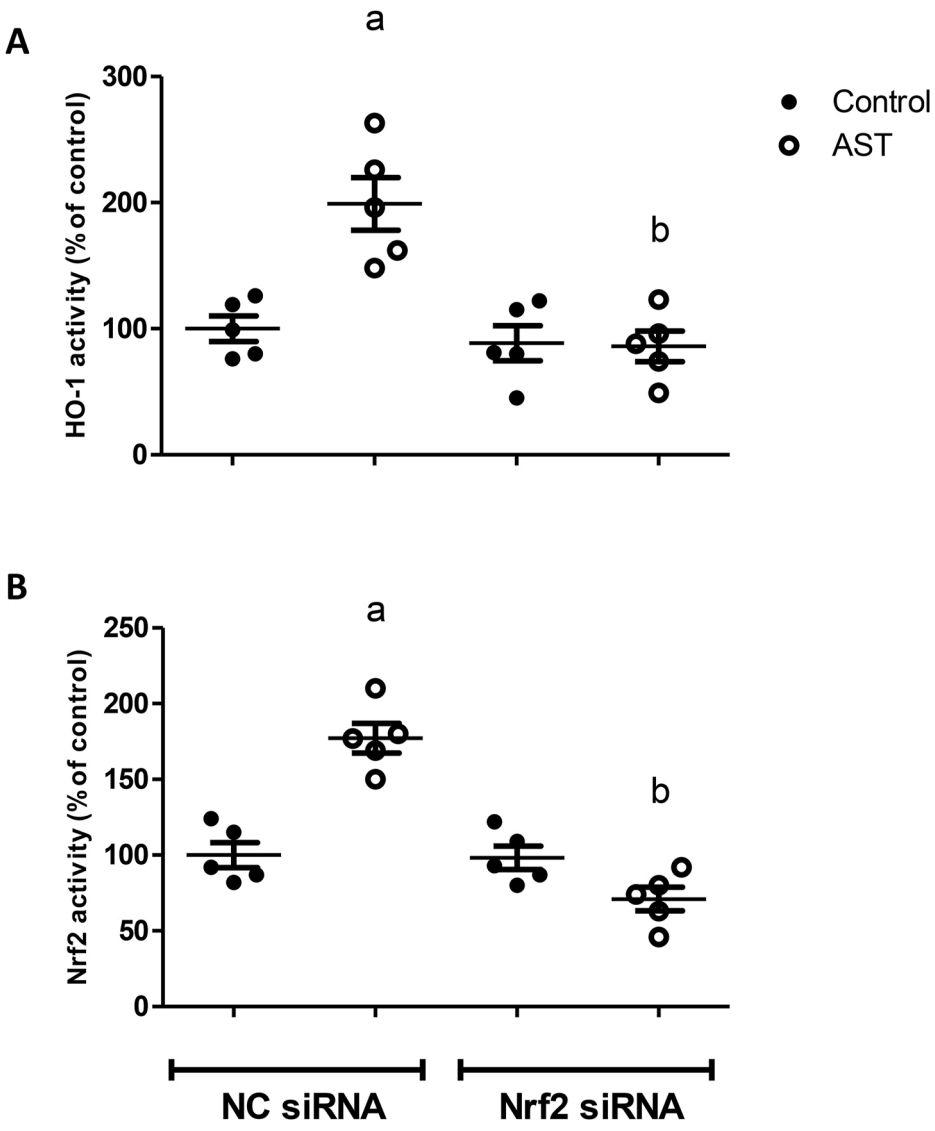

Fig. 10. The effects of astaxanthin (AST) and/or silencing of Nrf2 on the activity of the enzyme heme oxygenase-1 (HO-1) (A) and of Nrf2 (B). Silencing of the transcription factor Nrf2 was achieved by using small interfering RNA (siRNA) for 48 h prior to the treatment with AST at 20 μM. The data are presented as the mean ± S.E.M. of five independent experiments each done in triplicate. One-way ANOVA followed by the post hoc Tukey's test, a $p < 0.05$ vs control cells transfected with negative control (NC) siRNA, b $p < 0.05$ vs AST-treated cells transfected with NC siRNA.

HO-1 was not addressed in that work. Zhang et al. (2020) demonstrated that AST activates the Nrf2/HO-1 signaling pathway attenuating the effects of oxygen and glucose deprivation in SH-SY5Y cells. Interestingly, Lee et al. (2011) found that AST was not capable to modulate the activity of the antioxidant enzymes superoxide dismutase (SOD) and catalase (CAT) in SH-SY5Y cells. Moreover, Yan et al. (2016) reported that AST did not upregulate the levels of reduced glutathione (GSH, the major non-enzymatic antioxidant in animal cells) in the same cell line. SOD is the major enzyme involved in the conversion of $O_2^{-\bullet}$ into H_2O_2, and CAT generates water from H_2O_2 (Sies et al., 2017). Also, GSH is necessary to convert H_2O_2 into water in the reaction mediated by the enzyme GPx (Sies et al., 2017). Then, it is very likely that the activation of the Nrf2/HO-1 axis would be an important mechanism by which AST would be able to prevent redox and bioenergetics collapses in neuron-like cells. The involvement of other antioxidant enzymes in mediating the cytoprotective effects promoted by AST in brain cells should be further investigated.

Overall, the data presented here show that AST stimulated mitochondrial protection by a mechanism associated with the Nrf2/HO-1 axis. Further research would be useful to investigate whether other antioxidant enzymes, such as peroxiredoxins, for example, and other signaling pathways would be involved in the cytoprotection mediated by this xanthophyll. Furthermore, AST should be tested in *in vivo* experimental models, since natural molecules may present a low bioavailability in the mammalian organism.

Data availability statement

All data generated or analyzed during this study are included in this published article (and its supplementary information files).

Compliance with ethical standards funding

This study was funded by Conselho Nacional de Pesquisa e Desenvolvimento Tecnológico (CNPq) [grant number 301273/2018-9 (Bolsa de Produtividade em Pesquisa 2 - PQ2), and grant number 400216/2016-7]. Conflict of interest: the authors declare that they have no conflict of interest. Ethical approval: This article does not contain any studies with human participants or animals performed by any of the authors.

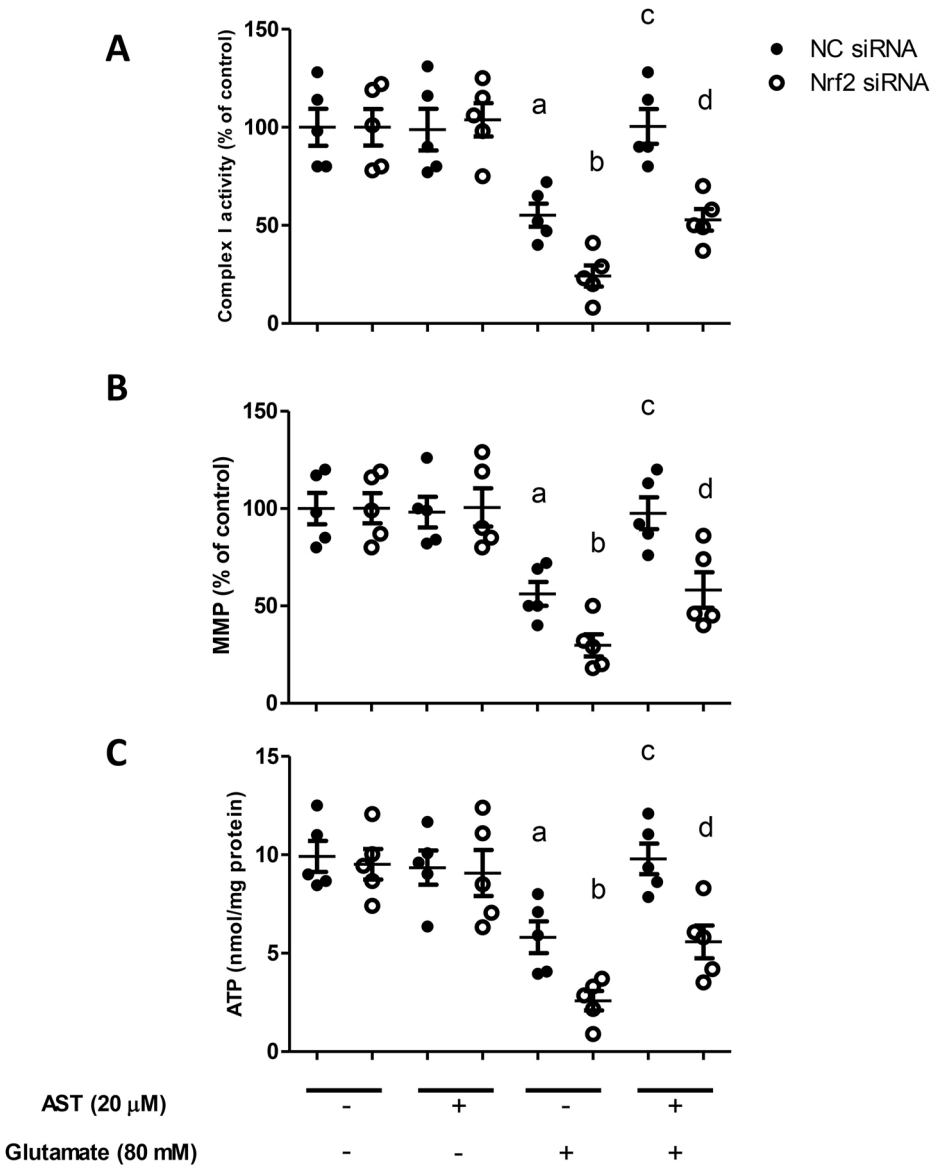

Fig. 11. The effects of silencing the transcription factor Nrf2 on the activity of Complex I (A), and on the levels of mitochondrial membrane potential (MMP) (B) and of adenosine triphosphate (ATP) (C) in the SH-SY5Y cells treated with astaxanthin (AST) and/or glutamate (GLU). Silencing of the transcription factor Nrf2 was achieved by using small interfering RNA (siRNA) for 48 h prior to the treatment with AST at 20 μM. The data are presented as the mean ± S.E.M. of five independent experiments each done in triplicate. One-way ANOVA followed by the post hoc Tukey's test, a $p < 0.05$ different from the control cells transfected with negative control (NC) siRNA; b $p < 0.05$ different from GLU-treated cells transfected with NC siRNA; c $p < 0.05$ different from GLU-treated cells transfected with NC siRNA; d $p < 0.05$ different from AST + GLU-treated cells transfected with NC siRNA.

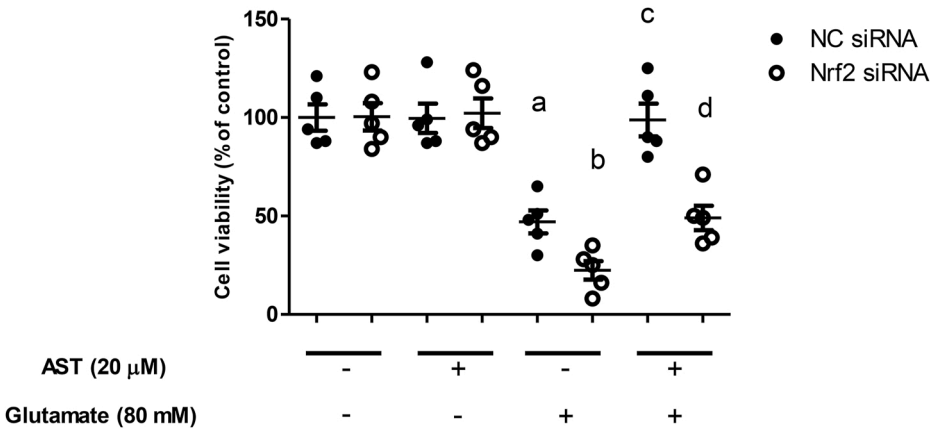

Fig. 12. The effects of silencing the transcription factor Nrf2 on the viability of the SH-SY5Y cells treated with astaxanthin (AST) and/or glutamate (GLU). Silencing of the transcription factor Nrf2 was achieved by using small interfering RNA (siRNA) for 48 h prior to the treatment with AST at 20 μM. The data are presented as the mean ± S.E.M. of five independent experiments each done in triplicate. One-way ANOVA followed by the post hoc Tukey's test, a $p < 0.05$ different from the control cells transfected with negative control (NC) siRNA; b $p < 0.05$ different from GLU-treated cells transfected with NC siRNA; c $p < 0.05$ different from GLU-treated cells transfected with NC siRNA; d $p < 0.05$ different from AST + GLU-treated cells transfected with NC siRNA.

CRediT authorship contribution statement

Flávia Bittencourt Brasil: Methodology, Formal analysis, Investigation, Writing – review & editing. **Fhelipe Jolner Souza de Almeida:** Methodology, Formal analysis, Investigation, Writing – review & editing. **Matheus Dargesso Luckachaki:** Methodology, Formal analysis, Investigation, Writing – review & editing. **Evandro Luiz Dall'Oglio:** Methodology, Writing – review & editing, Writing – review & editing. **Marcos Roberto de Oliveira:** Conceptualization, Methodology, Formal analysis, Investigation, Validation, Writing – original draft, preparation, Funding acquisition, Resources, Supervision, Project administration.

Declaration of competing interest

The authors declare that they have no known competing financial interests or personal relationships that could have appeared to influence the work reported in this paper.

Acknowledgments

MRO receives a "Bolsa de Produtividade em Pesquisa 2 - PQ2" fellow from the Conselho Nacional de Pesquisa e Desenvolvimento Tecnológico (CNPq) (protocol number 301273/2018-9). This work received financial support from CNPq (protocol number 400216/2016-7).

Appendix A. Supplementary data

Supplementary data related to this article can be found at https://doi.org/10.1016/j.ejphar.2021.174336.

References

Baranano, D.E., Rao, M., Ferris, C.D., Snyder, S.H., 2002. Biliverdin reductase: a major physiologic cytoprotectant. Proc. Natl. Acad. Sci. U.S.A. 99, 16093–16098. https://doi.org/10.1073/pnas.252626999.

Baranowski, C.J., 2018. The quality of life of older adults with epilepsy: a systematic review. Seizure 60, 190–197. https://doi.org/10.1016/j.seizure.2018.06.002.

Bonora, M., Patergnani, S., Rimessi, A., De Marchi, E., Suski, J.M., Bononi, A., Giorgi, C., Marchi, S., Missiroli, S., Poletti, F., Wieckowski, M.R., Pinton, P., 2012. ATP synthesis and storage. Purinergic Signal. 8, 343–357. https://doi.org/10.1007/s11302-012-9305-8.

Borutaite, V., Morkuniene, R., Brown, G.C., 1999. Release of cytochrome c from heart mitochondria is induced by high Ca2+ and peroxynitrite and is responsible for Ca(2+)-induced inhibition of substrate oxidation. Biochim. Biophys. Acta 1453, 41–48. https://doi.org/10.1016/s0925-4439(98)00082-9.

Cunha, M.P., Lieberknecht, V., Ramos-Hryb, A.B., Olescowicz, G., Ludka, F.K., Tasca, C. I., Gabilan, N.H., Rodrigues, A.L., 2016. Creatine affords protection against glutamate-induced nitrosative and oxidative stress. Neurochem. Int. 95, 4–14. https://doi.org/10.1016/j.neuint.2016.01.002.

de Oliveira, M.R., Ferreira, G.C., Schuck, P.F., Dal Bosco, S.M., 2015. Role for the PI3K/Akt/Nrf2 signaling pathway in the protective effects of carnosic acid against methylglyoxal-induced neurotoxicity in SH-SY5Y neuroblastoma cells. Chem. Biol. Interact. 242, 396–406. https://doi.org/10.1016/j.cbi.2015.11.003.

de Oliveira, M.R., Andrade, C.M.B., Fürstenau, C.R., 2018. Naringenin exerts anti-inflammatory effects in paraquat-treated SH-SY5Y cells through a mechanism associated with the Nrf2/HO-1 Axis. Neurochem. Res. 43, 894–903. https://doi.org/10.1007/s11064-018-2495-x.

de Oliveira, M.R., Duarte, A.R., Chenet, A.L., de Almeida, F.J.S., Andrade, C.M.B., 2019. Carnosic acid pretreatment attenuates mitochondrial dysfunction in SH-SY5Y cells in an experimental model of glutamate-induced excitotoxicity. Neurotox. Res. 36, 551–562. https://doi.org/10.1007/s12640-019-00044-8.

Duan, Y., Gross, R.A., Sheu, S.S., 2007. Ca2+-dependent generation of mitochondrial reactive oxygen species serves as a signal for poly(ADP-ribose) polymerase-1 activation during glutamate excitotoxicity. J. Physiol. 585, 741–758. https://doi.org/10.1113/jphysiol.2007.145409.

Fricker, M., Tolkovsky, A.M., Borutaite, V., Coleman, M., Brown, G.C., 2018. Neuronal cell death. Physiol. Rev. 98, 813–880. https://doi.org/10.1152/physrev.00011.2017.

Fürstenau, C.R., de Souza, I.C.C., de Oliveira, M.R., 2019. The effects of kahweol, a diterpene present in coffee, on the mitochondria of the human neuroblastoma SH-SY5Y cells exposed to hydrogen peroxide. Toxicol. Vitro 61, 104601. https://doi.org/10.1016/j.tiv.2019.104601.

Gao, X., He, D., Liu, D., Hu, G., Zhang, Y., Meng, T., Su, Y., Zhou, A., Huang, B., Du, J., Fu, S., 2020. Beta-naphthoflavone inhibits LPS-induced inflammation in BV-2 cells via AKT/Nrf-2/HO-1-NF-κB signaling axis. Immunobiology 225, 151965. https://doi.org/10.1016/j.imbio.2020.151965.

García, F., Lobos, P., Ponce, A., Cataldo, K., Meza, D., Farías, P., Estay, C., Oyarzun-Ampuero, F., Herrera-Molina, R., Paula-Lima, A., Ardiles, Á.O., Hidalgo, C., Adasme, T., Muñoz, P., 2020. Astaxanthin counteracts excitotoxicity and reduces the ensuing increases in calcium levels and mitochondrial reactive oxygen species generation. Mar. Drugs 18, 335. https://doi.org/10.3390/md18060335.

Gozzelino, R., Jeney, V., Soares, M.P., 2010. Mechanisms of cell protection by heme oxygenase-1. Annu. Rev. Pharmacol. Toxicol. 50, 323–354. https://doi.org/10.1146/annurev.pharmtox.010909.105600.

Hwang, Y.P., Kim, H.G., Han, E.H., Jeong, H.G., 2008. Metallothionein-III protects against 6-hydroxydopamine-induced oxidative stress by increasing expression of heme oxygenase-1 in a PI3K and ERK/Nrf2-dependent manner. Toxicol. Appl. Pharmacol. 231, 318–327. https://doi.org/10.1016/j.taap.2008.04.019.

Kausar, S., Wang, F., Cui, H., 2018. The role of mitochondria in reactive oxygen species generation and its implications for neurodegenerative diseases. Cells 7, 274. https://doi.org/10.3390/cells7120274.

Lee, D.H., Kim, C.S., Lee, Y.J., 2011. Astaxanthin protects against MPTP/MPP+-induced mitochondrial dysfunction and ROS production in vivo and in vitro. Food Chem. Toxicol. 49, 271–280. https://doi.org/10.1016/j.fct.2010.10.029.

Li, L., Chen, Y., Jiao, D., Yang, S., Li, L., Li, P., 2020a. Protective effect of astaxanthin on ochratoxin A-induced kidney injury to mice by regulating oxidative stress-related NRF2/KEAP1 pathway. Molecules 25, 1386. https://doi.org/10.3390/molecules25061386.

Li, X., Qin, X., Tian, J., Gao, X., Wu, X., Du, G., Zhou, Y., 2020b. Liquiritin protects PC12 cells from corticosterone-induced neurotoxicity via regulation of metabolic disorders, attenuation ERK1/2-NF-κB pathway, activation Nrf2-Keap1 pathway, and inhibition mitochondrial apoptosis pathway. Food Chem. Toxicol. 146, 111801 https://doi.org/10.1016/j.fct.2020.111801.

Ma, Q., 2013. Role of nrf2 in oxidative stress and toxicity. Annu. Rev. Pharmacol. Toxicol. 53, 401–426. https://doi.org/10.1146/annurev-pharmtox-011112-140320.

Madeira, V.M., 2012. Overview of mitochondrial bioenergetics. Methods Mol. Biol. 810, 1–6. https://doi.org/10.1007/978-1-61779-382-0_1.

Maines, M.D., 1990. Multiple forms of biliverdin reductase: age-related change in pattern of expression in rat liver and brain. Mol. Pharmacol. 38, 481–485.

Mohaghegh Shalmani, L., Valian, N., Pournajaf, S., Abbaszadeh, F., Dargahi, L., Jorjani, M., 2020. Combination therapy with astaxanthin and epidermal neural crest stem cells improves motor impairments and activates mitochondrial biogenesis in a rat model of spinal cord injury. Mitochondrion 52, 125–134. https://doi.org/10.1016/j.mito.2020.03.002.

Olloquequi, J., Cornejo-Córdova, E., Verdaguer, E., Soriano, F.X., Binvignat, O., Auladell, C., Camins, A., 2018. Excitotoxicity in the pathogenesis of neurological and psychiatric disorders: therapeutic implications. J. Psychopharmacol. 32, 265–275. https://doi.org/10.1177/0269881118754680.

Papa, S., Martino, P.L., Capitanio, G., Gaballo, A., De Rasmo, D., Signorile, A., Petruzzella, V., 2012. The oxidative phosphorylation system in mammalian mitochondria. Adv. Exp. Med. Biol. 942, 3–37. https://doi.org/10.1007/978-94-007-2869-1_1.

Poderoso, J.J., Carreras, M.C., Lisdero, C., Riobó, N., Schöpfer, F., Boveris, A., 1996. Nitric oxide inhibits electron transfer and increases superoxide radical production in rat heart mitochondria and submitochondrial particles. Arch. Biochem. Biophys. 328, 85–92. https://doi.org/10.1006/abbi.1996.0146.

Rego, A.C., Oliveira, C.R., 2003. Mitochondrial dysfunction and reactive oxygen species in excitotoxicity and apoptosis: implications for the pathogenesis of neurodegenerative diseases. Neurochem. Res. 28, 1563–1574. https://doi.org/10.1023/a:1025682611389.

Rieske, J.S., 1967. The quantitative determination of mitochondrial hemoproteins. Methods Enzymol. 10, 488–493.

Rochette, L., Zeller, M., Cottin, Y., Vergely, C., 2018. Redox functions of heme oxygenase-1 and biliverdin reductase in diabetes. Trends Endocrinol. Metabol. 29, 74–85. https://doi.org/10.1016/j.tem.2017.11.005.

Schmidt, D., Schachter, S.C., 2014. Drug treatment of epilepsy in adults. BMJ 348, g254. https://doi.org/10.1136/bmj.g254.

Sheeler, C., Rosa, J.G., Ferro, A., McAdams, B., Borgenheimer, E., Cvetanovic, M., 2020. Glia in neurodegeneration: the housekeeper, the defender and the perpetrator. Int. J. Mol. Sci. 21, 9188. https://doi.org/10.3390/ijms21239188.

Sies, H., Berndt, C., Jones, D.P., 2017. Oxidative stress. Annu. Rev. Biochem. 86, 715–748. https://doi.org/10.1146/annurev-biochem-061516-045037.

Sun, Z.W., Zhang, L., Zhu, S.J., Chen, W.C., Mei, B., 2010. Excitotoxicity effects of glutamate on human neuroblastoma SH-SY5Y cells via oxidative damage. Neurosci. Bull. 26, 8–16. https://doi.org/10.1007/s12264-010-0813-7.

Wakabayashi, N., Slocum, S.L., Skoko, J.J., Shin, S., Kensler, T.W., 2010. When NRF2 talks, who's listening? Antioxidants Redox Signal. 13, 1649–1663. https://doi.org/10.1089/ars.2010.3216.

Wang, H.Q., Sun, X.B., Xu, Y.X., Zhao, H., Zhu, Q.Y., Zhu, C.Q., 2010. Astaxanthin upregulates heme oxygenase-1 expression through ERK1/2 pathway and its protective effect against beta-amyloid-induced cytotoxicity in SH-SY5Y cells. Brain Res. 1360, 159–167. https://doi.org/10.1016/j.brainres.2010.08.100.

Wu, H., Niu, H., Shao, A., Wu, C., Dixon, B.J., Zhang, J., Yang, S., Wang, Y., 2015. Astaxanthin as a potential neuroprotective agent for neurological diseases. Mar. Drugs 13, 5750–5766. https://doi.org/10.3390/md13095750.

Yan, T., Zhao, Y., Zhang, X., Lin, X., 2016. Astaxanthin inhibits acetaldehyde-induced cytotoxicity in SH-SY5Y cells by modulating akt/CREB and p38MAPK/ERK signaling pathways. Mar. Drugs 14, 56. https://doi.org/10.3390/md14030056.

Zhang, J., Ding, C., Zhang, S., Xu, Y., 2020. Neuroprotective effects of astaxanthin against oxygen and glucose deprivation damage via the PI3K/Akt/GSK3β/Nrf2 signalling pathway in vitro. J. Cell Mol. Med. 24, 8977–8985. https://doi.org/10.1111/jcmm.15531.